Development 129, 551-561 (2002)
Printed in Great Britain © The Company of Biologists Limited 2002
DEV2769

Tail gut endoderm and gut/genitourinary/tail development: a new tissue-specific role for *Hoxa13*

Pascal de Santa Barbara and Drucilla J. Roberts*

Departments of Pathology and Pediatric Surgery Research, Massachusetts General Hospital, Harvard Medical School, Boston, MA 02114, USA
*Author for correspondence (e-mail: robertsd@helix.mgh.harvard.edu)

Accepted 11 November 2001

SUMMARY

Hoxa13 **is expressed early in the caudal mesoderm and endoderm of the developing hindgut. The tissue-specific roles of *Hoxa13* function have not been described. Hand-foot-genital syndrome, a rare dominantly inherited human malformation syndrome characterized by distal extremity and genitourinary anomalies, is caused by mutations in the *HOXA13* gene. We show evidence that one specific *HOXA13* mutation likely acts as a dominant negative in vivo. When chick *HFGa13* is overexpressed in the chick caudal endoderm early in development, caudal structural malformations occur. The phenotype is specific to *HFGa13* expression in the posterior endoderm, and includes taillessness and severe gut/genitourinary (GGU) malformations. Finally, we show that chick HFGa13 negatively regulates expression of *Hoxd13* and antagonizes functions of both endogenous Hoxa13 and Hoxd13 proteins. We suggest a fundamental role for epithelial specific expression of *Hoxa13* in the epithelial-mesenchymal interaction necessary for tail growth and posterior GGU patterning.**

Key words: *Hoxa13*, Tail, Endoderm, Gut, HFG, Chick

INTRODUCTION

Vertebrate gastrulation events form the three germ layers and pattern the early anterior body region. Although disputed, the posterior region probably forms via a separate secondary event at the undifferentiated mesenchyme of the tailbud to form the tail somites, distal neural tube, notochord and tailgut (Catala et al., 1995; Gajovic et al., 1993; Griffith et al., 1992; Holmdahl, 1925; Knezevic et al., 1998; Pasteels, 1943; Schoenwolf, 1977; Schoenwolf, 1979). A crucial early event in patterning the posterior embryo is the formation of the caudal intestinal portal (CIP), which initiates the development of the hindgut and tail, and forms the cloaca [the common gut/genitourinary (GGU) chamber]. The cloaca is maintained throughout life in avian and some other vertebrate species. In mammals, the cloaca exists as an embryonic structure that undergoes septation to become distinct urethral, anal, and genital orifices. Abnormal development of the cloaca causes severe congenital malformations in vertebrates, including humans (Kluth et al., 1995; Martinez-Frias et al., 2000).

Tail growth is a function of a specialized region of ectoderm, the ventral ectodermal ridge (VER), which acts analogously to the apical ectodermal ridge (AER) of the limb bud. Both the AER and VER signal adjacent mesodermal tissues to maintain an undifferentiated state, facilitating growth and elongation (Goldman et al., 2000; Saunders, 1948). The VER forms before morphological tail development [stage 18 in chick (Mills and Bellairs, 1989) and E10 or 35+ somites in the mouse (Gruneberg, 1956)] from the cloacal membrane posterior to the tailbud where ecotoderm and endoderm are juxtaposed (Gruneberg, 1956). During the ensuing gastrulation events, the tailgut develops anterior to the cloacal membrane and elongates in close association with the tail and in close proximity to its ectoderm. Apoptotic degeneration of the tailgut endoderm and VER heralds completion of tail growth (Fallon and Simandl, 1978; Miller and Briglin, 1996; Mills and Bellairs, 1989).

Despite common tail formation in early vertebrate development, tail growth ceases at different developmental time points in a species specific manner. Tail length is a characteristic phenotype among species, yet its molecular controls are unknown. Molecular candidates include the Hox genes [homeobox-containing transcription factors that function in many aspects of pattern formation during development (Krumlauf, 1994)]. In vertebrates, the Hox genes are expressed in a characteristic spatial and temporal pattern mirroring their physical location in the chromosome. The most 5′ Hox genes are expressed in the posterior body region including the posterior mesodermal regions of the gut (Roberts et al., 1995; Yokouchi et al., 1995b). These play an important role in patterning the gut along the anteroposterior axis (AP) (Roberts et al., 1995; Roberts et al., 1998; Warot et al., 1997). *Hoxa13* and *Hoxd13* are expressed specifically in the cloacal mesoderm and also uniquely in the hindgut and cloacal endoderm (Roberts et al., 1995; Yokouchi et al., 1995b). Their endodermal function is unknown.

Mutations in *Hoxa13*, both spontaneous and transgenic, exist in mice (Goodman and Scambler, 2001). The mutant phenotypes show both limb and GGU anomalies. Spontaneous murine *Hoxa13* mutant, hypodactyly (*hd*), has a 50 base deletion within the first exon of *Hoxa13*, resulting in a mutant fusion protein (Mortlock et al., 1996). Although these mice suffer a high perinatal mortality, some homozygotes survive but are infertile because of hypoplasia of distal reproductive structures (Warot et al., 1997). As the *Hoxa13*-null mice are early perinatal lethal (Fromental-Ramain et al., 1996), Hoxa13 protein may act as a gain-of-function mutant.

Murine *Hoxd13*$^{-/-}$ males show subtle GU anomalies (Dolle et al., 1993; Kondo et al., 1996; Podlasek et al., 1997) and have abnormalities of the lowest sacral vertebra (Dolle et al., 1993). *Hoxd13*$^{-/+}$ embryos crossed with *Hoxa13*-null heterozygotes, have more severe GGU anomalies than the *Hoxd13*$^{-/-}$ alone, suggesting that cooperation and redundancy between *Hoxa13* and *Hoxd13* exists in their function in GGU development (Warot et al., 1997).

Missense and nonsense mutations of one allele of *HOXA13* cause hand-foot-genital (HFG) syndrome (Goodman and Scambler, 2001), a rare, dominantly inherited human disease {OMIM 140000}. Affected individuals have mild, fully penetrant, symmetrical and bilateral hand and foot anomalies. Affected individuals also exhibit incompletely penetrant and variably severe GU tract abnormalities, including hypospadias in males and Müllerian duct fusion abnormalities in females. Both sexes show abnormalities in ureter/bladder placement. The variety of mutations described includes deletions, truncations of the protein, or amino acid substitutions within the conserved homeodomain. The resulting proteins are thought to act either as a gain-of-function mutation or as a possible competitor of the wild-type protein.

Mutations in human *HOXD13* cause a severe distal limb phenotype termed synpolydactyly (SPD) {OMIM 186000}. This rare, dominantly inherited syndrome is caused by mutations in a polyalanine repeat within the coding region of *HOXD13*, including expansions and intragenic deletions (Goodman and Scambler, 2001). Affected males often demonstrate GU abnormalities (Goodman and Scambler, 2001).

The manner in which these *HOXA13* and *HOXD13* mutations and nulls lead to these specific GGU malformations is unknown and may be due to mesodermal and/or endodermal effect of the mutation. To date, murine models have failed to address their possible tissue-specific functions.

To study the role of *Hoxa13* in GGU development we have used chick embryos. We have studied the specific endodermal role of *Hoxa13* using the avian specific retroviral expression system and in ovo electroporation to overexpress wild-type and mutant forms of *Hoxa13* in the chick hindgut endoderm in ovo. We constructed a chick *Hoxa13* homolog of one of the specific mutations that causes HFG (*HFGa13*). We chose the originally described *Hoxa13* mutation in which a small deletion in the C-terminal domain results in truncation of the protein (Morlock and Innis, 1997). When the truncated protein is expressed in the chick posterior endoderm, a dramatic GGU and tail malformation results. We show that this effect is specific to endodermal *HFGa13* expression. We show that HFGa13 probably acts by interfering with the normal function of endogenous Hoxa13 and Hoxd13.

MATERIALS AND METHODS

Embryos

Timed fertilized white leghorn eggs (SPAFAS, CT) were incubated at 38°C in a humidified incubator (Kuhl, NJ) until used experimentally. Embryos were staged according to Hamburger and Hamilton (Hamburger and Hamilton, 1951) or by embryonic day (E).

Constructs

Isolation of chicken *Hoxa13* gene has been previously described (Nelson et al., 1996). Although this clone was thought to be a full-length cDNA, a recent manuscript described evolutionarily conserved 3′ sequence which was not present in our original clone (Mortlock et al., 2000). We isolated this N-terminal sequence by RT-PCR on E6 hindgut total RNA with a primer designed to amplify the conserved 3′ sequence (ATGTTCCTCTACGACAACAGC). After sequence verification and subcloning we verified the full-length chick *Hoxa13* cDNA. By PCR, we mutated chick *Hoxa13* to produce a truncation similar to a specific human mutation (*HFGa13*). The mutated reverse oligonucleotide (TCAGATTGTGACCTGTCGC) produced a premature stop codon as described by Mortlock and Innis (Mortlock and Innis, 1997).

Wild-type *Hoxa13* and *HFGa13* cDNAs RCAS(A) or RCAS(B) viruses, and a *Hoxd13* RCAS(A) virus were produced as described (Morgan and Fekete, 1996). We found no difference in any of the experimental results described below using either the short or long form *Hoxa13* or *HFGa13*, and therefore we have not distinguished between them. Similarly, 3′ long and short forms of RCAS(A)*Hoxd13* acted equivalently in a chick limb bud overexpression study (Goff and Tabin, 1997). We found no difference in the infectivity of either A or B envelope coats of RCAS; both acted equivalently.

Constructs for electroporation were prepared with wild-type *Hoxa13* and *HFGa13* cDNAs cloned into pCDNA3 (Invitrogen). An N-Flag epitope oligonucleotide was inserted in frame with the GAL4 DNA-binding domain (Sadowski and Ptashne, 1989). All sequences were confirmed before use in experiments.

Transfection studies and western blots

Plasmids used for transfections were purified using the maxiprep reagent system (Qiagen). COS-7 cells at 60-80% confluence were washed twice with serum-free medium and then co-transfected with 100 ng of reporter plasmid [pG5*luc* containing 5 GAL4-binding sites (Promega)], 10 ng of Renilla luciferase promoter vector (Promega) and 100 ng of different *Hoxa13* plasmids with 3 μl of LipofectAMINE (Life Technologies) in 200 μl of serum-free medium. After 30 minutes of incubation, 500 μl of medium supplemented with 10% serum was added. Cells were harvested after 36 hours in culture. Luciferase assays were checked with the Dual-Luciferase^{TM} Reporter Assay (Promega). Promoter activities were expressed as relative luciferase activity (units/Renilla units) and each value represents the mean of six separate wells. Relative expression of the GAL4 fusion proteins was assessed by western blot analysis of COS-7 extracts. Transfections with wild-type *Hoxa13* and *HFGa13* constructs fused to GAL4 DNA-binding domain (DBD) were as described previously (Sadowski and Ptashne, 1989). GAL4 DBD antibody (Santa Cruz Biotech) was used as described by the manufacturer.

Cells were fixed 24 hours after transfection for 30 minutes in 4% paraformaldehyde in 0.1 M phosphate-buffered saline (PBS), permeabilized with PBS containing 0.02% Triton X-100, and incubated in 10% normal goat serum in PBS for 30 minutes at room temperature. Cells were then incubated with an anti-FLAG M5 monoclonal antibody (Kodak; 1:500) for 2 hours at room temperature, followed by incubation with secondary antibody. Images were collected and processed on a Microphot Nikon microscope.

Viral infection

This technique has been previously described (Morgan and Fekete,

1996). Embryos at stage 8-10 were used for experiments of the posterior endoderm, stage 18 for experiments in the limb. Approximately 1-5 μl of freshly defrosted virus dyed with Fast Green was injected per embryo. For hindgut experiments, the virus was injected into the region lateral and posterior to the tailbud after a published fate map (Matsushita, 1999). Double injections were performed by mixing equal volumes of each viral aliquot before injection, as previously described (Bendall et al., 1999). In all cases, the *HFGa13* virus was cloned in RCAS(B) and the wild-type viruses were in RCAS(A). For limb injections, the right hindlimb bud was viewed at stage 18. Approximately 1-5 μl of virus was injected, filling the entire limb bud. Eggs were then placed at 38°C until harvested. Injected viral constructs included short and long forms (see above) of wild-type *Hoxa13*, *HFGa13* and, as controls, wild-type *Hoxd13* and *GFP*. More than 10 dozen embryos were injected with each construct.

Electroporation

This technique was adapted to a technique previously published (Grapin-Botton et al., 2001). E2.5 (stage 11-14) embryos were used for electroporation, at CIP invagination and tailbud formation. Plasmids were diluted to a final concentration of 2 μg/ml in PBS adding 1 μM $MgCl_2$. To facilitate viewing of the viral aliquot and to slow diffusion, 50 μg/ml Nile Blue sulfate, 3 mg/ml carboxymethylcellulose was added to the construct liquid. This solution (5-10 μl) was deposited using a microcapillary pulled micropipette positioned under embryo at the posterior most endoderm layer (just caudal to the tailbud). Quickly after injection, a cathode was positioned on the dorsal surface of the embryo at the level of the injected construct. The anode was placed parallel to the cathode under the embryo (about 3 mm deep) at the level of the injected construct. Neither electrode touched the embryo. Three square pulses of 17 Volts and 50 mseconds each were applied to the embryo (BTX T-280 square wave electroporator generously lent to us by the Melton Lab under supervision of Anne Grapin-Botton) to allow vector integration into the endodermal layer. Eggs were incubated at 38°C until embryonic death or harvest. Controls included solution with all components except the vector, empty vector, vector constructed with wild-type *Hoxa13* or with vector constructed with *GFP*. Approximately three dozen eggs were electroporated in experimental and control groups.

Whole embryo explants

The technique was adapted from that of Chapman et al. (Chapman et al., 2001). Dissected stage 9-13 embryos were placed ventral side up in a freshly made thin layer of albumin/agarose (Chapman et al., 2001). Using a dissecting microscope (Olympus SZH10), the posterior endoderm covering the tailbud and posterior was removed using one of these techniques: dissection alone using pulled glass needles and fine forceps, enzymatic digestion using 0.03% collagenase in PBS dropped on the embryo over the tailbud and allowed to sit for 15 minutes at 37°C and washed with five drop/aspirate cycles using PBS+10% chick serum followed by five drop/aspirate cycles using PBS+pen/strep or a combination of both techniques. Controls had no manipulation. Transplanted embryos had caudal endoderm removed as above. Donor endoderm was removed from donor stage 17 embryos (for facility and to ensure good *Hoxa13* expression by the posterior endoderm) by sharp dissection, kept oriented and divided into thirds along the AP axis. The anterior endoderm and posterior endoderm were isolated and transplanted to host embryos (separately) by transfer pipette and forceps. Embryos were harvested immediately after manipulation, and at 24 and 48 hours. For each condition, at least 12 embryos were used over five separate experiments.

Analysis

Embryos were harvested and fixed in freshly made 4% paraformaldehyde in PBS for 4-20 hours. Fixed embryos were washed in PBS and then either taken through a graded series of methanol-PBS washes and kept at –20°C in methanol until used for whole-mount in situ hybridization studies or for cyrosections. Whole-mount in situ hybridization studies followed our published technique (Roberts et al., 1998). Cryosections (10 μm) on Superfrost Plus slides (Fisher Scientific) were air dried for 4-18 hours and kept at –20°C until used. Some fixed, in situ hybridized embryos were embedded in paraffin and sectioned at 5 μm for histological analysis. Hematoxylin and Eosin staining was performed using standard techniques. Section in situ hybridization was performed using published techniques (Smith et al., 2000). Immunohistochemical stains were performed using standard techniques and the Vectastain ABC detection system (Vector Laboratories) following the manufacturer's directions. Hoxa13 antibody was a generous gift from A. Kuroiwa and used as previously described (Yokouchi et al., 1995a). 3C2 antibody specific to RCAS GAG protein has been published before (Smith et al., 2000). Ribroprobes were transcribed using Roche ribroprobe synthesis kits as per the manufacturer's directions. All riboprobes used herein have been previously published (Nielsen et al., 2001; Roberts et al., 1995; Roberts et al., 1998; Smith et al., 2000; Vogel et al., 1996).

Accession numbers

GenBank Accession Number for *Gallus gallus Hoxa13* is AY030050.

RESULTS

Spatiotemporal expression of *Hoxa13* during posterior GGU/tail development

Hoxa13 is first expressed early in the most posterior part of the embryo, adjacent to Hensen's node in the area that will give rise to the CIP (stage 10) **(**Fig. 1A**)**. *Hoxa13* is expressed at stage 14 in the CIP (Fig. 1B). Later, *Hoxa13* expression is restricted to the dorsal mesoderm of the tailbud, cloacal mesoderm, hindlimb bud mesoderm and caudal endoderm **(**Fig. 1C,D**)**. *Hoxa13* and its product are strongly expressed in the endoderm of the hindgut and cloaca through early development of the gut (Fig. 1E,F) (Roberts et al., 1995; Yokouchi et al., 1995b).

Human HFG and chick HFGa13 overexpressed embryos have similar phenotypes

Overexpression of *Hoxa13* in the posterior embryo failed to produce a tail or gut phenotype. We did see an epithelial transformation (from midgut to hindgut) when midgut mesodermal tissues expressed *Hoxa13* (see Fig. 7H for comments) as was described with ectopic *Hoxd13* expression in the midgut (Roberts et al., 1998).

To determine if expression of chick mutated *Hoxa13* (*HFGa13*) results in a phenotype similar to that observed in the human HFG syndrome, we chose to construct a similar nonsense mutation as described by Mortlock and Innis (Mortlock and Innis, 1997). The C-terminal mutation leads to a mutated Hoxa13 protein with the last 20 last amino acids deleted. We expected that HFGa13 protein would be able to interfere with the endogenous Hoxa13.

In order to test our hypothesis, we first misexpressed *HFGa13* in the hindlimb, and we were able to produce a severe morphological change reminiscent of the limb defect described in HFG syndrome **(**Fig. 2A**)**. The *HFGa13*-expressing hindlimb showed a specific malformation characterized by a substantial reduction in limb size in both the anteroposterior and dorsoventral axes compared with the uninfected contralateral control limb. *HFGa13* E6 infected hindlimbs revealed a specific skeletal hypoplasia of the fibula (without changes in the tibia) and a reduction of the entire autopod area

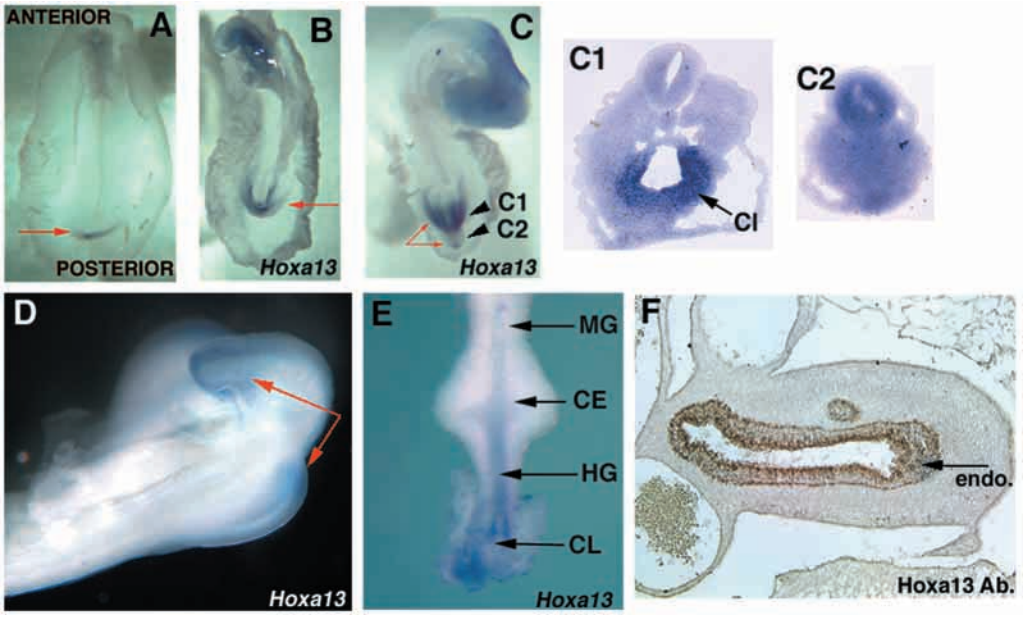

Fig. 1. Spatiotemporal expressions of *Hoxa13* (A-E) and Hoxa13 protein (F) during posterior GGU/tail development. (A) Stage 10 [arrow indicates caudal intestinal portal (CIP)]. (B) Stage 14 (arrow indicates CIP). (C) Stage 17 (long arrows show tail tip and hindgut, arrowheads at tail gut). C1 and C2 note planes of cryosection. (C1) *Hoxa13* endodermal expression in the cloaca (Cl). (D) Expression in tail and posterior hindlimb bud (red arrows) at stage 22. (E) Dissected E4 posterior gut. Expression is present in the hindgut (HG) and cloacal (CL) endoderm and cloacal mesoderm, no expression is detected in the ceca (CE) or midgut (MG). (F) Protein expression in hindgut endoderm (endo.), arrow, at E6.

(Fig. 2A,B). This phenotype suggested a late disruption of the apical ectodermal ridge (AER). Consistent with this, *Fgf8* mRNA expression (Vogel et al., 1996) was not detectable in the distal hindlimb AER of the *HFGa13* hindlimbs **(**Fig. 2C**)**. The distal fibular cartilage fails to properly develop and remains undifferentiated. Expression of *Bapx1* was decreased only in the malformed fibula **(**Fig. 2D**)**. No AER disruption or fibula maldevelopment were observed with the wild-type *Hoxa13* overexpression (data not shown). These results suggest that *HFGa13* interferes with the maintenance of the AER in the hindlimb and with formation of the fibula. We conclude that our construct functions to give a chick phenocopy of the human HFG syndrome.

Endodermally expressed *HFGa13* causes abnormal hindgut and tail development

HFGa13 and control constructs were expressed in the chick in ovo by injection of virus, targeting the prospective hindgut in stage 8-10 embryos. We used this targeting technique previously to infect the midgut mesoderm (Roberts et al., 1998), but in the

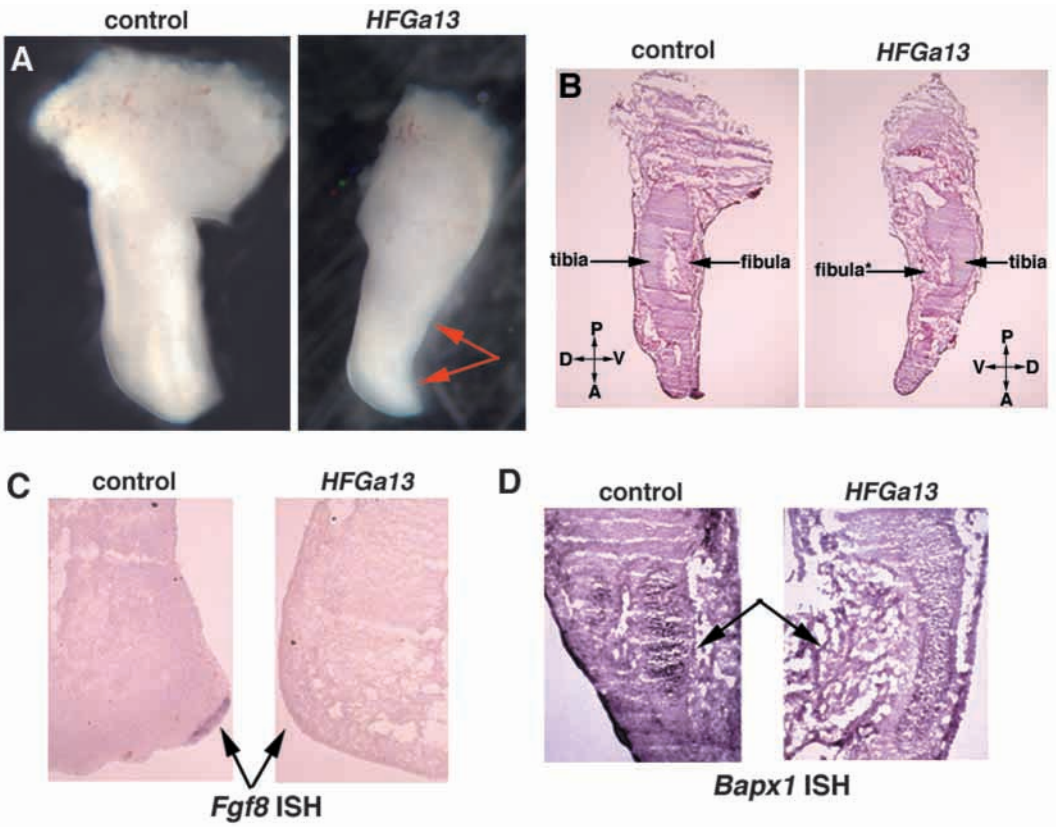

Fig. 2. Human hand-foot-genital (HFG) and chick *HFGa13* overexpressed embryos have similar limb phenotypes. (A-D) Control (left panel) and *HFGa13*-infected (right panel) hindlimbs at E6. Planar sections of E6 limbs (B), uninjected control (left) *HFGa13*-infected hindlimb [right, arrows indicate fibula maldevelopment (fibula*) with undifferentiated mesenchymal cells]. (C) In situ hybridization of *Fgf8* in sectioned hindlimb. No *Fgf8* expression is detected in the *HFGa13*-infected hindlimb compared with the uninfected hindlimb (arrows). (D) In situ hybridization of *Bapx1* in sectioned hindlimb. There is altered *Bapx1* expression in the *HFGa13*-infected hindlimb (arrows).

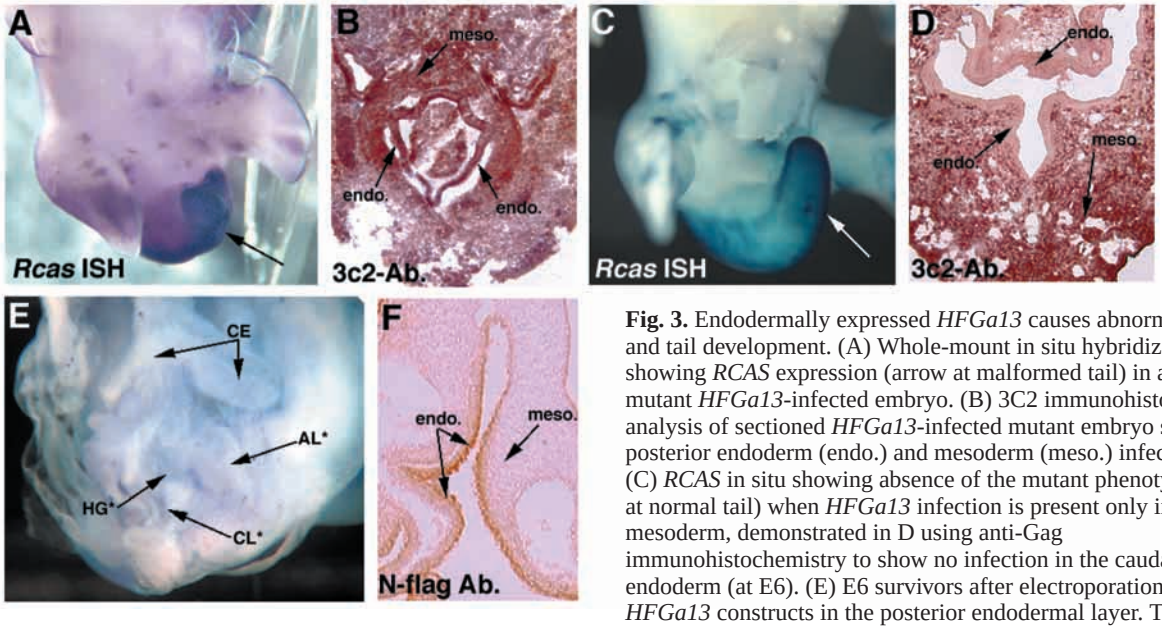

Fig. 3. Endodermally expressed *HFGa13* causes abnormal hindgut and tail development. (A) Whole-mount in situ hybridization showing *RCAS* expression (arrow at malformed tail) in an E6 mutant *HFGa13*-infected embryo. (B) 3C2 immunohistochemistry analysis of sectioned *HFGa13*-infected mutant embryo shows posterior endoderm (endo.) and mesoderm (meso.) infection. (C) *RCAS* in situ showing absence of the mutant phenotype (arrow at normal tail) when *HFGa13* infection is present only in the mesoderm, demonstrated in D using anti-Gag immunohistochemistry to show no infection in the caudal endoderm (at E6). (E) E6 survivors after electroporation of *HFGa13* constructs in the posterior endodermal layer. The phenotype involves maldevelopment of the cloaca (CL*), hindgut (HG*) and tail. Allantoic internalization is present (AL*) and ceca are unaffected (CE). (F) Anti-N-flag immunostaining demonstrating expression of the tagged-HFGa13 in the endoderm of the hindgut; the mesoderm is not stained. Note that the electroporated endodermal cells appear undamaged and intact. Misexpression of *HFGa13* and *Hoxa13* constructs by electroporation show similar expression levels in the gut endoderm layer (data not shown).

experiments described herein we often found strong endodermal infection in the hindgut as well **(**Fig. 3B**)**.

Specific gross morphological defects were obtained only with *HFGa13* infections and only when the infection included the posterior endoderm (Fig. 3A,B). *Hoxa13*, *Shh*, *Bmp4* and *GFP* constructs always failed to produce this phenotype ever, even when expression was noted in the endoderm (data not shown). *HFGa13* embryos infected specifically in the mesoderm only were phenotypically normal (Fig. 3C,D). Our survival rate was 50-80%, depending on time of incubation (survival to E3 better than to E18). Approximately 20% of *HFGa13*-injected embryos demonstrated the mutant phenotype. All *HFGa13* embryos were analyzed for viral infection. All mutant embryos harbored posterior endodermal and mesodermal virus expression. Those without the phenotype showed no viral infection or only posterior mesodermal virus expression (no infection in the endoderm).

To determine if endodermal expression of *HFGa13* is sufficient to obtain these posterior defects we used an in ovo electroporation technique (Grapin-Botton et al., 2001). Three groups of E2.5 (stage 11-16) embryos were electroporated: a control group with empty vector or a *GFP*-containing vectors, a group with the wild-type *Hoxa13* construct and a group with *HFGa13*. In E5 survivors, posterior short tail/hindgut atresia was present only in the *HFGa13* electroporated embryos, whereas electroporation of control constructs produced no defects (data not shown). The mutant phenotype was restricted to those embryos with hindgut epithelial expression of *HFGa13* [electroporations restricted to the midgut endoderm failed to produce the posterior phenotype (data not shown)]. Survival was about 80% for all groups. The posterior endodermal *HFGa13* expressing embryos show similar, albeit more severe, defects as those obtained using the injection/infection technique (Fig. 3E). Confirmation of tissue integration and endodermal tissue survival were performed by tag immunostaining on all embryos **(**Fig. 3F**)**. Sections of experimental embryos confirmed an intact endoderm and a histologically normal neural tube and notochord (Fig. 4).

Approximately 10 embryos (all the survivors and all the embryos with documented expression in the hindgut endoderm) showed the phenotype that included malformations of the hindgut and tail (Fig. 4A,C,E,G), including maldevelopment of the tail somites and a short tail (compare Fig. 4A,C, respectively, with Fig. 4B,D). Hindgut defects included hindgut atresia anterior to the cloaca (Fig. 4E,F) and malformed/malpositioned cloacas (compare Fig. 4C,E, respectively, with Fig. 4D,F). Additional defects were noted in other cloaca-associated viscera, including cystic mesonephric maldevelopment with normal non-atretic ureters and atresia of the distal Müllerian ducts (Fig. 4G,H). No associated neural tube defects or malformations are present (as shown in Fig. 4). We occasionally obtained a severe phenotype, termed ourentery (Rabaud, 1900), in which the tail appears to have grown ventrally and internally to the remaining cloacal orifice, often accompanied with ventral internal malpositioning of tail structures into the hindgut and internalization of the allantois (compare Fig. 4A,C with Fig. 4B,D and also Fig. 3B with Fig. 3D).

HFGa13 affects expression of *Hoxd13*, *Fgf8* and *Bapx1*

Molecular analyses of *HFGa13* mutant embryos were made with specific dorsoventral (DV), anteroposterior (AP) and cytodifferentiation markers. Strong downregulation was observed with VER marker *Fgf8* (ectoderm and mesoderm) and with AP marker *Hoxd13* (mesoderm and endoderm) (Fig. 5A and Fig. 5D, respectively**)**. *Bapx1* shows a diminished expression in the short tail **(**Fig. 5B**)**. No change was noted in the expression

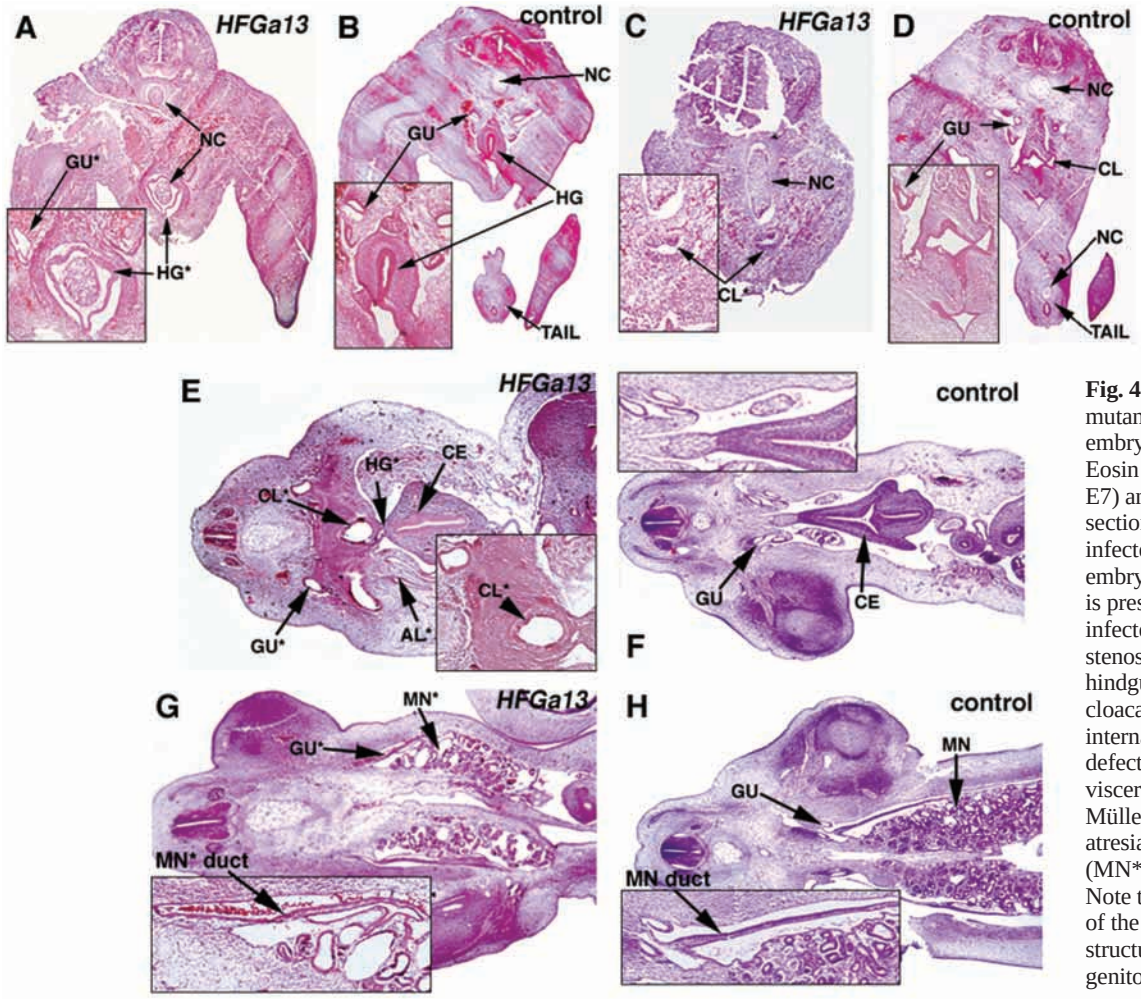

Fig. 4. Histological analysis of mutant *HFGa13*-infected embryos. Hematoxylin and Eosin stained transverse (A-D; E7) and longitudinal (E-H; E6) sections of mutant *HFGa13*-infected (A,C,E,G) and control embryos (B,D,F,H). Ourentery is present in A. *HFGa13*-infected embryos show cloacal stenosis (CL*; C), atresia of the hindgut (HG*) anterior to the cloaca (CL; E), allantoic internalization (AL*; E) and defects in the cloaca-associated viscera, including more distal Müllerian duct (MN duct) atresia and cystic mesonephric (MN*) maldevelopment (G). Note the correct development of the more anterior gut structures. CE, ceca; GU, genitourinary; NC, notocord.

of ventral mesodermal markers *Wnt5a* **(**Fig. 5C) and *Bmp4* (data not shown), and there was normal expression of *Shh* **(**Fig. 5E**)**.

Caudal gut endodermal signals are needed for normal posterior gut and tail development

To test our hypothesis that posterior gut and tail development requires specific endodermal signals, we used whole embryo explant cultures in which we removed the endoderm at early (pre-CIP) stages (stage 9-11). Survival (90% of unmanipulated controls, 75% of manipulated embryos) after 2 days, to stage 20, allowed analysis of tail development. None of the control embryos had caudal defects (Fig. 6A). All embryos in which the caudal endoderm had been removed showed severe caudal defects of the tail and gut. Those embryos that survived to form hindlimb buds generally formed abnormal CIP and blunted tails similar to those produced in the *HFGa13*-injected or electroporated embryos **(**Fig. 6B**)**. Ourentery was present in 50% of manipulated survivors **(**Fig. 6D**)**. No neural tube defect was present in these embryos.

When examined histologically, we confirmed that the midline ventral endoderm overlying the tailbud was removed (data not shown). This endoderm is absent for the first 24 hours after dissection, then it appears that the adjacent endoderm occasionally re-grows over this defect (Fig. 6D). No defects are seen in the more anterior endoderm (Fig. 6C). To confirm that removal of the caudal endoderm was complete, we analyzed the normal and abnormal embryos for the presence of early endodermal markers. In the caudal ventral tissues of normal embryos, we found expression of *Shh*, *CdxA* (Fig. 6E), *Hoxa13* (Fig. 6A) and *Hoxd13* (data not shown). However, we could not detect expression of these markers in the caudal ventral tissues of abnormal embryos before 24 hours **(**Fig. 6B,F**)**. Rescue experiments included transplanting donor endoderm (either anterior or posterior) harvested from stage 17 embryos to the embryos in which the CIP endoderm had been removed. Only transplanted posterior endoderm rescued the tail and gut defect (Fig. 6G). Anterior endodermal transplants failed to rescue blunted tail phenotype (Fig. 6H). Our results show that the posterior endoderm produces signals necessary for normal tail and hindgut development.

HFGa13 interferes with the cellular functions of Hoxa13 and Hoxd13 proteins

To investigate the molecular pathway by which HFG *Hoxa13* mutation functions, transactivation activities of wild-type Hoxa13 and HFGa13 were first analyzed in heterologous COS-7 cell line by luciferase assay using the synthetic GAL4 reporter system. Constructions for transfection studies were prepared using the pSG424 vector that contains the GAL4 DNA-binding domain. Wild-type *Hoxa13*, *HFGa13* and *Hoxd13* cDNAs were subcloned into pSG424 vector in frame with the GAL4 DBD. We show that wild-type Hoxa13 protein

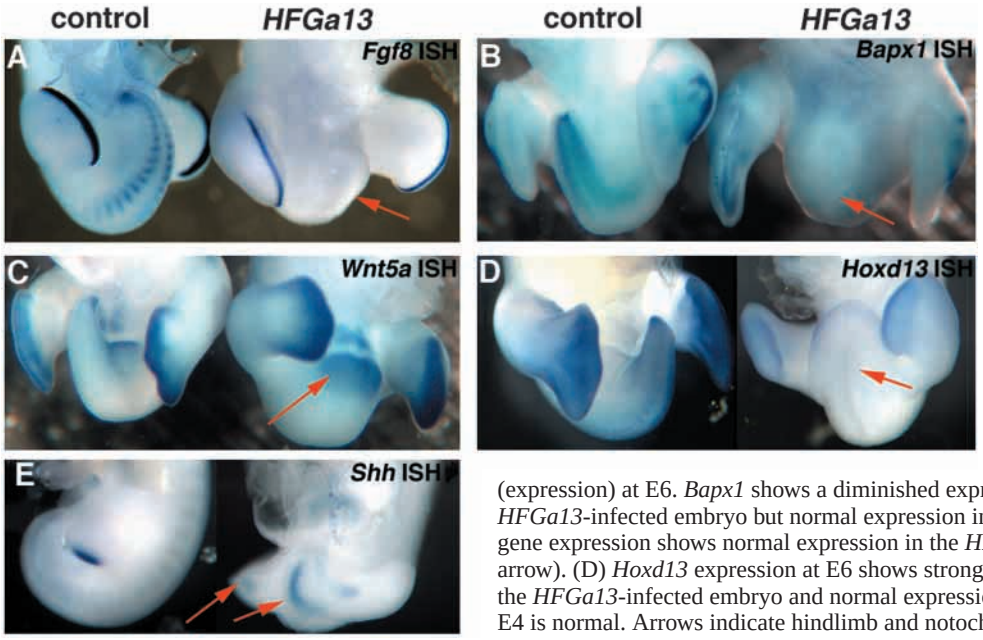

Fig. 5. *HFGa13* affects expression of *Fgf8*, *Hoxd13* and *Bapx1*. (A-E) Whole-mount in situ hybridization of control (left panel) and *HFGa13*-infected (right panel) embryos (arrows at malformed tail). (A) *Fgf8* expression at E5, note absence of expression in the HFGa13 tail (red arrow) but normal expression in the hindlimb AER. (B) *Bapx1* (expression) at E6. *Bapx1* shows a diminished expression in the tail (red arrow) of the *HFGa13*-infected embryo but normal expression in the non-infected hindlimbs. (C) *Wnt5a* gene expression shows normal expression in the *HFGa13*-infected embryo at E7 (red arrow). (D) *Hoxd13* expression at E6 shows strong downregulation in the tail (red arrow) of the *HFGa13*-infected embryo and normal expression in hindlimbs. (E) *Shh* expression at E4 is normal. Arrows indicate hindlimb and notochord.

fused to the GAL4 DNA-binding domain is able to activate transcription of this synthetic reporter **(**Fig. 7A**)**. The HFGa13 construct is not able to activate the synthetic GAL4 promoter but we did notice a decrease in the basal activity using this construct. To verify expression and protein stability, we performed western blot analysis on whole COS-7 cell extracts of transfected cells using a specific GAL4 DBD antibody. We show that all these proteins were expressed at comparable levels, as assayed by western blotting, indicating that the inability to activate transcription is not linked to a lack of expression or instability of the HFGa13 proteins **(**data not shown**)**. To determine whether a difference in intracellular localization of HFGa13 proteins could affect transcriptional activity, localization of N-flag-tagged proteins within transfected COS-7 cells was examined by immunostaining **(**Fig. 7C,D**)**. Strong signals for wild-type Hoxa13 and HFGa13 proteins were observed in the nuclei of transfected COS-7 cells.

Using the same synthetic GAL4 reporter system, we investigated the possible interactions between Hoxa13 and HFGa13. We used the same conditions with a plasmid containing *Hoxa13* and a GAL4 DBD, but added one plasmid containing *HFGa13* cDNA without GAL4 DBD (unable to bind the 5 GAL4 DBD repeats). Using this competition assay with same molar ratio, we show that HFGa13 protein is able to decrease *Hoxa13* transcriptional activity (Fig. 7B). Increased amounts of HFGa13 increase the strength of the repression (data not shown). Interestingly, HFGa13 protein is also able to act in a dominant negative fashion with Hoxd13 by repressing Hoxd13 transcriptional activity (Fig. 7B).

In order to determine if *HFGa13* acts as a dominant negative in vivo we used a competitive assay taking advantage of an epithelial phenotype alteration induced by overexpression of the wild-type *Hoxa13* in the midgut. At E18, epithelial differentiation is nearly complete. Midgut epithelium is characterized by long and thin villi (Fig. 7E), whereas hindgut epithelium shows wide and flat villi (Fig. 7F). We have previously shown that ectopic *Hoxd13* expression in the midgut mesoderm causes the midgut epithelium to develop with a hindgut/cloacal phenotype (Roberts et al., 1998). We now show that the same epithelial transformation occurs with *Hoxa13* misexpression in the midgut mesoderm (Fig. 7H,J). However, infection of the midgut with *HFGa13* did not transform the epithelium (Fig. 7G). If our *HFGa13* acts as a dominant negative, then it should be able to repress the midgut epithelial transformation induced by ectopic midgut mesodermal *Hoxa13* or *Hoxd13* expression. In order to test our hypothesis, we co-infected mesodermal midgut with either RCAS(A)-*Hoxa13* or *Hoxd13* and RCAS(B)-*HFGa13* in equal titer/volume. We used the different RCAS envelope proteins to facilitate cellular co-infection as previously described (Morgan and Fekete 1996; Bendall et al., 1999). To verify co-infection, we checked viral expression in the midgut mesoderm by 3c2 immunostaining, and we deduced co-expression of either *Hoxa13* or *Hoxd13* and *HFGa13* by in situ hybridization probing with the wild-type probes (Fig. 7L). Co-expression of *HFGa13* with *Hoxa13* (Fig. 7I) or with *Hoxd13* (Fig. 7K) was sufficient to inhibit the action of *Hoxa13* or *Hoxd13*. As we found wild-type epithelium phenotype in the co-infected mesoderm midguts, we can deduce that *HFGa13* must have acted as a dominant negative.

These experiments indicate that this HFG nonsense mutation probably functions as a dominant negative. HFGa13 may compete with the endogenous function of wild-type Hoxa13 and/or Hoxd13 proteins in vivo as a dominant-negative, as observed with humans heterozygous for this mutation, probably by interfering with protein partners and/or transcriptional machinery.

DISCUSSION

It has been known for some time that there is a close association between the development of the gut and the tail or its related structures (coccyx and sacral vertebrae). Human congenital malformations in one often affect the other systems. This association is seen in spontaneous and transgenic

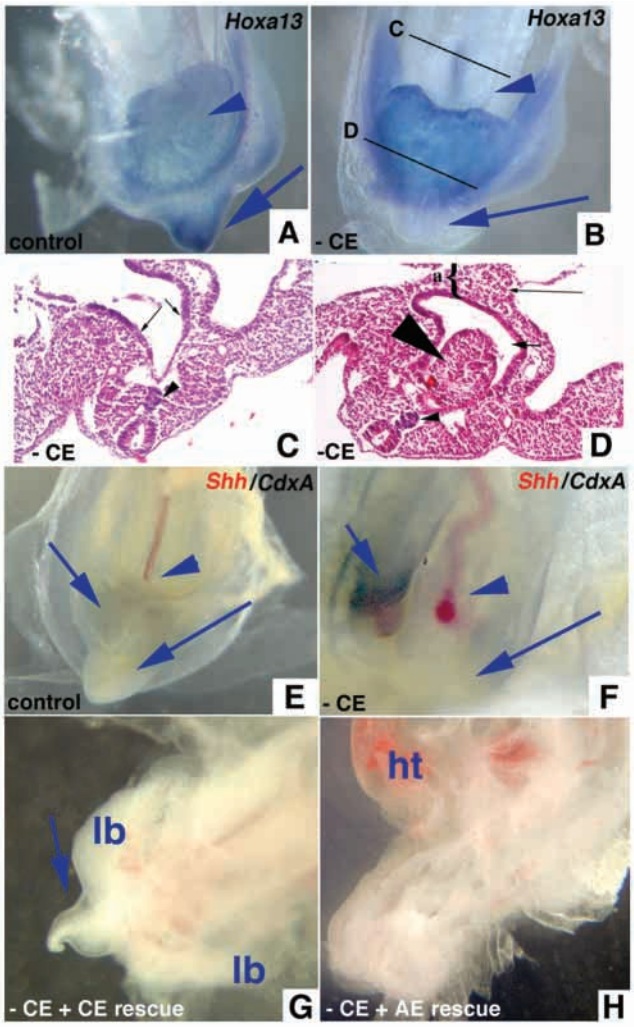

Fig. 6. Whole embryo explants developed in culture demonstrate the physical necessity of caudal endoderm for normal tail development. (A) Whole embryo explanted at stage 10 and grown on albumen/agarose for 48 hours, showing normal tail development and expression of *Hoxa13* in tail (blue arrow). Arrowhead shows normal placement of allantois ventral to hindgut, which expresses *Hoxa13*. (B) Stage 10 embryo grown with caudal endoderm removed, demonstrating blunted tail without *Hoxa13* expression (arrow). Arrowhead indicates hindgut dorsal to *Hoxa13*-expressing allantois. Location of sections shown in C,D are indicted. (C) Anterior section of caudal endoderm-less embryo as in B, showing normal endoderm (arrows) and notochord (arrowhead). (D) Hematoxylin and Eosin stained section through a caudal endoderm-less embryo that developed ourentery (large arrowhead) within hindgut lumen (short arrow). The bracket and long arrow indicate allantois. Small arrowhead indicates normal notochord. (E) Embryo cultured for ~24 hours with caudal endoderm develops normal CIP (long arrow), expresses *Shh* in notochord (red stain, arrowhead, most of notochord deep to plane of photograph) and co-expresses *Shh* and *CdxA* in endoderm of CIP (short arrow, purple/black stain). (F) Embryo cultured for ~24 hours without caudal endoderm fails to develop CIP or express *Shh* or *CdxA* in midline caudal endoderm (long arrow), both are co-expressed in right lateral caudal endoderm (short arrow, purple/black stain). Notochord is curved but expresses *Shh* (red stain, arrowhead). (G) Embryo after caudal endoderm removed and donor caudal endoderm transplanted, cultured for ~48 hours showing tail growth (arrow). lb, hindlimb buds. (H) Embryo after caudal endoderm removed and donor anterior endoderm transplanted, cultures at ~48 hours showing blunted tail (long arrow), allantois (arrowhead); AE, anterior endoderm; –CE, caudal endoderm removed; ht, heart.

malformations in many vertebrate species (Maatman et al., 1997; Warot et al., 1997). The GGU and tail tissues derive from the tailbud mesenchyme probably via secondary body formation (Griffith et al., 1992). The factors involved in this process, if mutated, may affect multiple caudal structures. There is evidence to support this, both experimentally and spontaneously produced, in many vertebrate systems. When regions of the tailbud are removed early in chick development, tail truncations and cloacal anomalies are common (Schoenwolf, 1978). In some specific spontaneous murine mutants with tail truncation anomalies, GGU malformations are common. For example, Danforth's short tail mutant (*sd*) develops anal stenosis, rectal duplications and anal atresias in association with the characteristic short tail (Dunn et al., 1940). In humans, the relationship between sacral and coccygeal vertebral defects and hindgut defects has also been documented (van der Putte, 1986) in sporadic/isolated malformations [e.g. cloacal and bladder exstrophy (Loder and Dayioglu, 1990; Martinez-Frias et al., 2000)] and syndromic malformations [e.g. VATERCL syndrome that includes anal atresia and hemivertebrae (Beals and Rolfe, 1989)]. Another example is the limb/pelvis-hypoplasia/aplasia syndrome that includes absent fibulae, Müllerian aplasia and sacral hypoplasia (Raas-Rothschild et al., 1988). The elucidation of the mechanism of this association has been difficult, probably owing to the complexity of the malformations. As the malformations often involve anomalies of all three germ layers, deciphering the primary from the secondary effects in a transgenic model is troublesome.

Tail development is universal among vertebrates, although the persistence of a tail is not. Tail length is a function of the developmental time point when tailgut and VER apoptosis occurs. We suggest a functional relationship between the caudal endoderm and the VER. Gruneberg suggested that the origin of the VER is from the cloacal membrane (Gruneberg, 1956). Other experimental evidence supports the association between caudal endoderm and the VER. VER ablation causes a displacement of the tailgut dorsally, by increasing the number of cells between the VER and tailgut (Goldman et al., 2000). In murine chimeras derived from wild-type and *sd* mutant ES cells, it was shown that the *sd* cells never populated the ventral hindgut or tailgut, suggesting a ventral signal from the gut endoderm is absent in the *sd* mutant mouse (Maatman et al., 1997). It may be that the failure of heterozygous and homozygous *sd* mutant cells to colonize the ventral hindgut endoderm is the earliest manifestation of the *sd* phenotype (Maatman et al., 1997).

The molecular controls of normal or abnormal tail/GGU are poorly understood, but VER function and signals have recently been described (Goldman et al., 2000). Signals from specialized ectoderm in the limb (AER) and the tail (VER) direct elongation of their respective subjacent structures. The AER and VER do not appear to be functionally equivalent. In mice, both the AER and VER express a fibroblast growth factor and a bone morphogenic protein (Dudley and Tabin, 2000; Maatman et al., 1997). Although exogenous application of FGF or BMP to the AER rescues the limb phenotype in AER

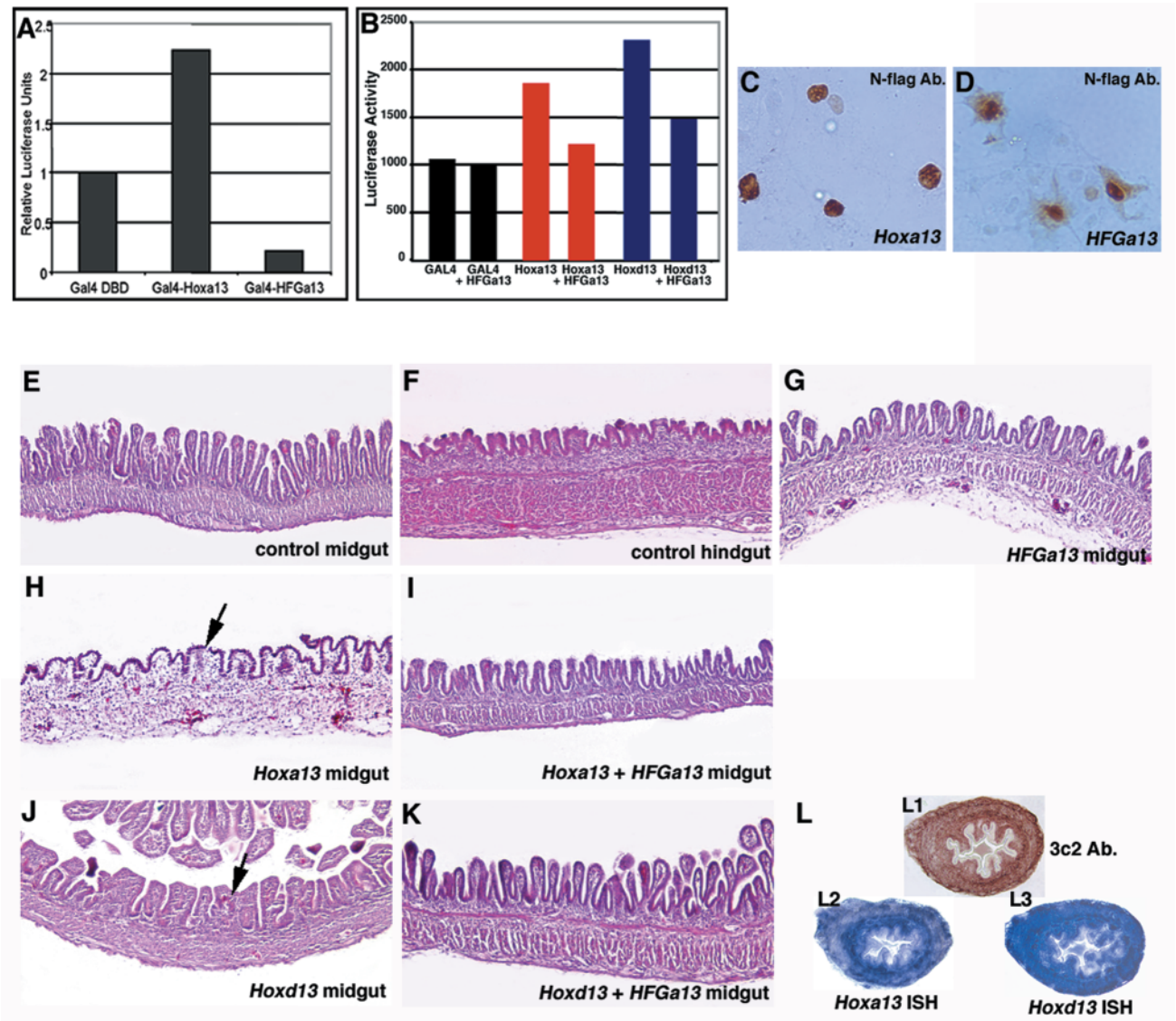

Fig. 7. HFGa13 interferes with the cellular functions of Hoxa13 and Hoxd13. (A) Transcriptional transactivation by wild-type Hoxa13 and HFGa13 proteins in a GAL4-fusion assay in COS-7 cells. Relative luciferase activities were normalized to the empty GAL4 DNA-binding domain expression vector. Fusion protein of the GAL4 DNA-binding domain and Hoxa13 shows transcriptional activation of the synthetic reporter. By contrast, fusion protein of the GAL4 DNA-binding domain and HFGa13 fails to activate transcription of the same promoter and is able to decrease the basal activity. Luciferase assays were performed after two independent transfections, each done in triplicate (A,B). (B) Perturbation of the transcriptional transactivation of wild-type Hoxa13 and Hoxd13 by HFGa13 in a GAL4-fusion assay in COS-7 cells. In this assay, we monitored GAL4 transcriptional activity induced by GAL4 DBD fusion proteins without or with pcDNA3-HFGa13 construct. In a same molar ratio, the HFGa13 form specifically decreases Hoxa13 and Hoxd13 transcriptional activation. (C,D) Intracellular localization of Hoxa13 and HFGa13 proteins. Immunostaining of transfected N-flag tagged Hoxa13 (C) and HFGa13 (D) constructs in COS-7 cells with specific N-flag antibody shows that both have nuclear localization. Note an additive cytoplasmic signal with the HFGa13 construct. (E-K) Hematoxylin and Eosin stained sections of E18 control (E,F) or infected (G-K) guts. (E) Normal midgut with thin and long villi. (F) Normal hindgut with flat and short villi. (G) *HFGa13* mesodermally infected midgut has wild-type midgut epithelium. *Hoxa13* (H) and *Hoxd13* (J) mesodermally infected midgut shows hindgut-like epithelial transformation (as shown by arrows). *HFGa13* midguts co-infected with either *Hoxa13* (I) or *Hoxd13* (K) show rescue of the epithelial hindgut phenotype. (L) *Hoxd13* and *HFGa13* mesodermal midgut co-infection show presence of virus (detected by 3C2-Ab, L1), and ectopic *HFGa13* (detected with *Hoxa13* probe, L2) and *Hoxd13* (L3) co-expression, which is associated with normal epithelial phenotype.

ablated embryos (Zuniga et al., 1999), when these proteins were placed on VER ablated tails in vitro, they failed to rescue the blunted tail phenotype (Goldman et al., 2000). Transplanting the AER to VER ablated tails also fails in rescuing growth (Goldman et al., 2000). There are clearly other factors, either from the VER or other tail tissues, that are important in directing tail development. We conclude that signaling between the endoderm and ectoderm at this very early stage of development is critical and independent of notochord or neural tube related inductions. We suggest that one of these factors is *Hoxa13* derived from the caudal endoderm.

Clearly, there are multiple factors involved in tail development. Many different model systems (genetic, mechanical and toxic) can result in the phenotype of blunted tail and cloacal anomalies. Classical anatomic literature has examples of toxic or pharmacological induction of blunted tail and ourenteric malformations in chick, including exposure to insulin (Moseley, 1947), organophosphides (Wyttenbach and Thompson, 1985) and retinoic acid (Griffith and Wiley, 1989). Mechanical disruptions by transection or extirpation of the notochord, tailbud and hindgut endoderm, shaking, or placement of a conductive glass tube all result in blunted tail and ourentery (Moseley, 1947; Hotary and Robinson, 1992). The transgenic data in mice shows that pertubations in many different pathways result in blunted tails including FGF (Furthauer et al., 1997), BMP (Brunet et al., 1998), Wnt (Yamaguchi et al., 1999) and retinoic acid (Abu-Abed et al., 2001). What is common to these diverse 'methods' of producing the combination of caudal tail/vertebrae and gut defects? We suggest one possibility may be interruption of caudal endoderm signaling needed for normal tail development.

A spontaneous genetically dominant chicken mutation resembles the phenotype of our *HFGa13* embryos. Dominant rumpless chicks develop a truncated tail and abnormal cloaca, and often show ourentery (Zwilling, 1942). It would be very interesting to determine if *Hoxa13* is mutated or if abnormalities in this pathway are present in this strain. We are currently studying dominant rumpless chick embryos for *Hoxa13* mutations.

In the human syndrome HFG, no sacral or coccygeal anomalies have been reported. In the murine counterpart, *hd* shows anal stenosis but not caudal vertebrae or tail defects (Post and Innis, 1999). Interestingly, caudal vertebrate malformations due to mutations in the paralog *Hoxd13*, though, have been reported both in human SPD syndrome (Akarsu et al., 1996) and in homozygous *Hoxd13* knockout mice (Dolle et al., 1993). We show that our HFGa13 construct interferes with the normal expression and function of *Hoxd13* **(**Fig. 5, Fig. 7**)**. Our *HFGa13* phenotype may be in part an indirect phenomenon that is due to downregulation of *Hoxd13*.

It is curious that the human, chick and murine phenotypes differ given the same genetic alteration. It may be that there are subtle vertebral defects in human individuals with HFG not described to date. Similarly, subtle murine lumbosacral or tail abnormalities may have escaped observation in the *hd* or *Hoxa13*$^{-/-}$ mice. Our findings in chick may relate to the particular *Hoxa13* mutation we constructed or to the relative levels of wild-type and mutant proteins in the 'transgenic' embryos. Or, it may be due to a different function of *Hoxa13* in avian species in the posterior vertebrae compared with that of mouse and human.

A theory derived from our results suggests that the presence of a tail structure in a vertebrate species may be related to persistence of the tailgut during development. In humans and avians the tailgut undergoes apoptotic regression relatively early in development (Fallon and Simandl, 1978; Miller and Briglin, 1996), whereas in rodents the tailgut persists over a much longer relative developmental time period (Goldman et al., 2000). Although this study does not address the upstream controls of *Hoxa13* expression in this caudal region, it follows that significant differences in this control should exists among species with different tail lengths.

We thank C. Nielsen, S. Winfield and T. Manganaro for excellent technical assistance; C. Tabin and P. Donahoe for generous guidance, use of reagents and expertise; and G. Schoenwolf, L. Pierro and F. Goldman for helpful discussions and insights into our results. We are especially appreciative of direct guidance and sharing of equipment from D. Melton and A. Grapin-Botton. We are indebted to A. Kuroiwa and his laboratory for generous sharing of the precious Hoxa13 antibody. Thanks to Sandrine Faure and Alexandre de Santa Barbara for support. This work was supported by NIH grant HD34448-03 to D. J. R. P. d. S. B. is supported by an ARC postdoctoral fellowship and an American Foundation for Urology Diseases Fellowship Grant.

REFERENCES

Abu-Abed, S., Dolle, P., Metzger, D., Beckett, B., Chambon, P. and Petkovich, M. (2001). The retinoic acid-metabolizing enzyme, CYP26A1, is essential for normal hindbrain patterning, vertebral identity, and development of posterior structures. *Genes Dev.* **15**, 226-240.

Akarsu, A. N., Stoilov, I., Yilmaz, E., Sayli, B. S. and Sarfarazi, M. (1996). Genomic structure of HOXD13 gene: a nine polyalanine duplication causes synpolydactyly in two unrelated families. *Hum. Mol. Genet.* **5**, 945-952.

Beals, R. K. and Rolfe, B. (1989). VATER association. A unifying concept of multiple anomalies. *J. Bone Joint Surg. Am.* **71**, 948-950.

Bendall, A. J., Ding, J., Hu, G., Shen, M. M. and Abate-Shen, C. (1999). Msx1 antagonizes the myogenic activity of Pax3 in migrating limb muscle precursors. *Development* **126**, 4965-4976.

Brunet, L. J., McMahon, J. A., McMahon, A. P. and Harland, R. M. (1998). Noggin, cartilage morphogenesis, and joint formation in the mammalian skeleton. *Science* **280**, 1455-1457.

Catala, M., Teillet, M. A. and Le Douarin, N. M. (1995). Organization and development of the tail bud analyzed with the quail- chick chimaera system. *Mech. Dev.* **51**, 51-65.

Chapman, S. C., Collignon, J., Schoenwolf, G. C. and Lumsden, A. (2001). Improved method for chick whole-embryo culture using a filter paper carrier. *Dev. Dyn.* **220**, 284-289.

Dolle, P., Dierich, A., LeMeur, M., Schimmang, T., Schuhbaur, B., Chambon, P. and Duboule, D. (1993). Disruption of the Hoxd-13 gene induces localized heterochrony leading to mice with neotenic limbs. *Cell* **75**, 431-441.

Dudley, A. T. and Tabin, C. J. (2000). Constructive antagonism in limb development. *Curr. Opin. Genet. Dev.* **10**, 387-392.

Dunn, L., Gluecksohn-Schoenheimer, S. and Bryson, V. (1940). A new mutation in the mouse affection spinal column and urogenital system. *J. Hered.* **31**, 343-348.

Fallon, J. F. and Simandl, B. K. (1978). Evidence of a role for cell death in the disappearance of the embryonic human tail. *Am. J. Anat.* **152**, 111-129.

Fromental-Ramain, C., Warot, X., Messadecq, N., LeMeur, M., Dolle, P. and Chambon, P. (1996). Hoxa-13 and Hoxd-13 play a crucial role in the patterning of the limb autopod. *Development* **122**, 2997-3011.

Furthauer, M., Thisse, C. and Thisse, B. (1997). A role for FGF-8 in the dorsoventral patterning of the zebrafish gastrula. *Development* **124**, 4253-4264.

Gajovic, S., Kostovic-Knezevic, L. and Svajger, A. (1993). Morphological evidence for secondary formation of the tail gut in the rat embryo. *Anat. Embryol.* **187**, 291-297.

Goff, D. J. and Tabin, C. J. (1997). Analysis of Hoxd-13 and Hoxd-11 misexpression in chick limb buds reveals that Hox genes affect both bone condensation and growth. *Development* **124**, 627-636.

Goldman, D. C., Martin, G. R. and Tam, P. P. (2000). Fate and function of the ventral ectodermal ridge during mouse tail development. *Development* **127**, 2113-2123.

Goodman, F. R. and Scambler, P. J. (2001). Human HOX gene mutations. *Clin. Genet.* **59**, 1-11.

Grapin-Botton, A., Majithia, A. R. and Melton, D. A. (2001). Key events of pancreas formation are triggered in gut endoderm by ectopic expression of pancreatic regulatory genes. *Genes Dev.* **15**, 444-454.

Griffith, C. M. and Wiley, M. J. (1989). Direct effects of retinoic acid on the development of the tail bud in chick embryos. *Teratology* **39**, 261-75.

Griffith, C. M., Wiley, M. J. and Sanders, E. J. (1992). The vertebrate tail bud: three germ layers from one tissue. *Anat. Embryol.* **185**, 101-113.

Gruneberg, H. (1956). A ventral ectodermal ridge of the tail in mouse embryos. *Nature* **177**, 787-788.
Hamburger, V. and Hamilton, H. L. (1951). A series of normal stages in the development of the chick embryo. *J. Morphol.* **88**, 49-92.
Holmdahl, D. E. (1925). Experimentelle untersuchungen uber die lage der grenze zwischen primarer and sekundarer korperentwicklung beium huhn. *Anat. Anz Bd* **59**, 393-396.
Hotary, K. B. and Robinson, K. R. (1992). Evidence of a role for endogenous electrical fields in chick embryo development. *Development* **114**, 985-996.
Kluth, D., Hillen, M. and Lambrecht, W. (1995). The principles of normal and abnormal hindgut development. *J. Pediatr. Surg.* **30**, 1143-1147.
Knezevic, V., De Santo, R. and Mackem, S. (1998). Continuing organizer function during chick tail development. *Development* **125**, 1791-1801.
Kondo, T., Dolle, P., Zakany, J. and Duboule, D. (1996). Function of Posterior *HoxD* genes in the morphogenesis of the anal sphincter. *Development* **122**, 2651-2659.
Krumlauf, R. (1994). Hox genes in vertebrate development. *Cell* **78**, 191-201.
Loder, R. T. and Dayioglu, M. M. (1990). Association of congenital vertebral malformations with bladder and cloacal exstrophy. *J. Pediatr. Orthop.* **10**, 389-393.
Maatman, R., Zachgo, J. and Gossler, A. (1997). The Danforth's short tail mutation acts cell autonomously in notochord cells and ventral hindgut endoderm. *Development* **124**, 4019-4028.
Martinez-Frias, M. L., Bermejo, E. and Rodriguez-Pinilla, E. (2000). Anal atresia, vertebral, genital, and urinary tract anomalies: a primary polytopic developmental field defect identified through an epidemiological analysis of associations. *Am. J. Med. Genet.* **95**, 169-173.
Matsushita, S. (1999). Fate mapping study of the endoderm in the posterior part of the 1.5-day- old chick embryo. *Dev. Growth Differ.* **41**, 313-319.
Miller, S. A. and Briglin, A. (1996). Apoptosis removes chick embryo tail gut and remnant of the primitive streak. *Dev. Dyn.* **206**, 212-218.
Mills, C. L. and Bellairs, R. (1989). Mitosis and cell death in the tail of the chick embryo. *Anat. Embryol.* **180**, 301-308.
Morgan, B. A. and Fekete, D. M. (1996). Manipulating gene expression with replication-competent retroviruses. In *Methods in Avian Embryology*. Vol. 51 (ed. M. Bronner-Fraser), pp. 185-218. San Diego: Academic Press.
Mortlock, D. P. and Innis, J. W. (1997). Mutation of HOXA13 in hand-foot-genital syndrome. *Nat. Genet.* **15**, 179-180.
Mortlock, D. P., Post, L. C. and Innis, J. W. (1996). The molecular basis of hypodactyly (Hd): a deletion in Hoxa 13 leads to arrest of digital arch formation. *Nat. Genet.* **13**, 284-289.
Mortlock, D. P., Sateesh, P. and Innis, J. W. (2000). Evolution of N-terminal sequences of the vertebrate HOXA13 protein. *Mamm. Genome* **11**, 151-158.
Moseley, H. R. (1947). Insulin-induced remplessness of chickens IV. Early embryology. *J. Exp. Zool.* **105**, 279-316.
Nelson, C. E., Morgan, B. A., Burke, A. C., Laufer, E., DiMambro, E., Murtaugh, L. C., Gonzales, E., Tessarollo, L., Parada, L. F. and Tabin, C. (1996). Analysis of Hox gene expression in the chick limb bud. *Development* **122**, 1449-1466.
Nielsen, C., Murtaugh, L. C., Chyung, J. C., Lassar, A. and Roberts, D. J. (2001). Gizzard formation and the role of Bapx1. *Dev. Biol.* **231**, 164-174.
Pasteels, J. (1943). Proliférations et croissance dans la gastrulation et la formation de la queue des vertébrés. *Arch. Biol.* **54**, 1-51.
Podlasek, C. A., Duboule, D. and Bushman, W. (1997). Male accessory sex organ morphogenesis is altered by loss of function of Hoxd-13. *Dev. Dyn.* **208**, 454-465.
Post, L. C. and Innis, J. W. (1999). Infertility in adult hypodactyly mice is associated with hypoplasia of distal reproductive structures. *Biol. Reprod.* **61**, 1402-1408.
Raas-Rothschild, A., Goodman, R. M., Meyer, S., Katznelson, M. B., Winter, S. T., Gross, E., Tamarkin, M., Ben-Ami, T., Nebel, L. and Mashiach, S. (1988). Pathological features and prenatal diagnosis in the newly recognised limb/pelvis-hypoplasia/aplasia syndrome. *J. Med. Genet.* **25**, 687-697.
Rabaud, E. (1900). Etude embryologique de l'ourentérie et de la cordentérie. *J. L'Anat. Physiol.* 619-634.
Roberts, D. J., Johnson, R. L., Burke, A. C., Nelson, C. E., Morgan, B. A. and Tabin, C. (1995). Sonic hedgehog is an endodermal signal inducing Bmp-4 and Hox genes during induction and regionalization of the chick hindgut. *Development* **121**, 3163-3174.
Roberts, D. J., Smith, D. M., Goff, D. J. and Tabin, C. J. (1998). Epithelial-mesenchymal signaling during the regionalization of the chick gut. *Development* **125**, 2791-2801.
Sadowski, I. and Ptashne, M. (1989). A vector for expressing GAL4(1-147) fusions in mammalian cells. *Nucleic Acids Res.* **17**, 7539.
Saunders, J. W. (1948). The proximo-distal sequence of the origin of the parts of the chick wing and the role of the ectoderm. *J. Exp. Zool.* **108**, 363-403.
Schoenwolf, G. C. (1977). Tail (end) bud contributions to the posterior region of the chick embryo. *J. Exp. Zool.* **201**, 227-246.
Schoenwolf, G. C. (1978). Effects of complete tail bud extirpation on early development of the posterior region of the chick embryo. *Anat. Rec.* **192**, 289-295.
Schoenwolf, G. C. (1979). Histological and ultrastructural observations of tail bud formation in the chick embryo. *Anat. Rec.* **193**, 131-147.
Smith, D. M., Nielsen, C., Tabin, C. J. and Roberts, D. J. (2000). Roles of BMP signaling and Nkx2.5 in patterning at the chick midgut-foregut boundary. *Development* **127**, 3671-3681.
van der Putte, S. C. (1986). Normal and abnormal development of the anorectum. *J. Pediatr. Surg.* **21**, 434-440.
Vogel, A., Rodriguea, C., Izpisua-Belmonte, J. C. (1996). Involvement of FGF-8 in initiation, outgrowth and patterning of the vertebrate limb. *Development* **122**, 1737-1750.
Warot, X., Fromental-Ramain, C., Fraulob, V., Chambon, P. and Dolle, P. (1997). Gene dosage-dependent effects of the Hoxa-13 and Hoxd-13 mutations on morphogenesis of the terminal parts of the digestive and urogenital tracts. *Development* **124**, 4781-4791.
Wyttenbach, C. R. and Thompson, S. C. (1985). The effects of the organophosphate insecticide malathion on very young chick embryos: malformations detected by histological examination. *Am. J. Anat.* **174**, 187-202.
Yamaguchi, T. P., Bradley, A., McMahon, A. P. and Jones, S. (1999). A Wnt5a pathway underlies outgrowth of multiple structures in the vertebrate embryo. *Development* **126**, 1211-1223.
Yokouchi, Y., Nakazato, S., Yamamoto, M., Goto, Y., Kameda, T., Iba, H. and Kuroiwa, A. (1995a). Misexpression of Hoxa-13 induces cartilage homeotic transformation and changes cell adhesiveness in chick limb buds. *Genes Dev.* **9**, 2509-2522.
Yokouchi, Y., Sakiyama, J. and Kuroiwa, A. (1995b). Coordinated expression of Abd-B subfamily genes of the HoxA cluster in the developing digestive tract of chick embryo. *Dev. Biol.* **169**, 76-89.
Zuniga, A., Haramis, A. P., McMahon, A. P. and Zeller, R. (1999). Signal relay by BMP antagonism controls the SHH/FGF4 feedback loop in vertebrate limb buds. *Nature* **401**, 598-602.
Zwilling, E. (1942). The development of dominant rumplessness in chick embryos. *Genetics* **27**, 641-656.